

HARMONIC RESONANCE RISK ANALYSIS AND THE EFFECTS OF ADVANCED CONTROL AND COORDINATION IN HIGH PV PENETRATION NETWORKS

SERHAT ISIKLI

Global Enco Energy and Technology Inc., Atlanta, GA, USA. ORCID ID: 0009-0006-2507-0656

Abstract

This study analyzes the mechanisms of harmonic resonance formation in distribution systems with high photovoltaic (PV) penetration and its impact on system stability, power quality, and protection reliability. The growing integration of PV units alters system impedance due to inverter-based power electronics, leading to stronger resonance and harmonic interactions. The IEEE 13-bus distribution system was used as a reference model, and MATLAB/Simulink-based simulations were performed to conduct frequency scans, harmonic load flow, and transient analyses under varying PV penetration levels (10%, 30%, 50%). Results show that higher PV ratios cause downward shifts in resonance frequencies, increase total harmonic distortion (THD), and heighten the risk of protection relay malfunctions. Active damping and virtual impedance-based control strategies effectively mitigate these issues, reducing resonance peaks by up to 50%. The study emphasizes the need for coordinated power quality and protection planning in high PV penetration networks.

Keywords: Photovoltaic Penetration, Harmonic Resonance, Power Quality, Protection Coordination, Active Damping Control.

1. INTRODUCTION

Renewable energy sources have become a pivotal component of global electricity generation over the past decades. Among these sources, photovoltaic (PV) systems have emerged as a key technology due to their cost-effectiveness, flexible deployment capabilities, and high technological maturity (Gandhi et al., 2020; Sampath Kumar et al., 2020). The widespread adoption of PV-based generation units has transformed the structure of electricity networks from centralized to distributed architectures, thereby altering the impedance profile, power flow characteristics, and dynamic stability of traditional distribution systems (Chidurala et al., 2015).

PV inverters employ power electronic switches to convert direct current (DC) into alternating current (AC). During this conversion process, switching actions generate harmonic components at multiples of the fundamental frequency. These harmonics interact with the grid impedance and the reactive elements within the network, potentially triggering resonance phenomena at specific frequencies (Kalair et al., 2017; Eroğlu et al., 2021). Resonance occurs when the system impedance attains a maximum or minimum at certain frequencies, resulting in small harmonic currents inducing large voltage distortions (Liang et al., 2021). Such distortions degrade power quality and can lead to the unintended operation of protection devices (Kaddah et al., 2015).

Historically, distribution systems were dominated by passive loads and a limited number of capacitor banks. However, with the increasing integration of inverter-based PV

resources, the surrounding network impedance has decreased, resonance frequencies have shifted toward lower ranges, and harmonic interactions have intensified (Zhao et al., 2022). These effects are particularly pronounced in systems containing capacitor banks, where capacitive reactance interacts with inverter-side inductances to form resonant conditions (Farzin & Monadi, 2022). For example, in a typical LCL filter configuration, the resonance frequency can be expressed as:

$$f_{res} = \frac{1}{2\pi} \sqrt{\frac{L_1 + L_2}{L_1 L_2 C}}$$

where L_1 and L_2 represent the inverter- and grid-side inductances, respectively, and C denotes the filter capacitance. Improper selection of these parameters may shift the resonance frequency toward higher-order harmonics, thereby adversely affecting system stability (Hosseinpour et al., 2023).

As PV systems continue to proliferate, issues related to harmonic resonance and stability at the distribution level have become increasingly significant (De Rua et al., 2023). Luo et al. (2015) demonstrated that in large-scale PV plants, resonance frequencies exhibit a nonlinear relationship with inverter filter parameters. Similarly, Zeng et al. (2019) showed that virtual resistance-based control strategies can reduce resonance peak amplitudes by up to 40%. However, most existing studies have primarily focused on power quality aspects, while the interaction between resonance and protection systems has received limited attention (Barutcu et al., 2019).

During resonance events, measurement filters within protection relays may fail to adequately suppress harmonic components, leading to inaccuracies in RMS calculations and resulting in maloperation (false tripping) or underreach (failure to trip) conditions (Müller et al., 2020). Liu & Molinas (2020) reported that inverter digital delays can alter harmonic current amplitudes, causing deviations of up to 15% in relay threshold settings. These findings highlight that PV systems introduce new technical challenges that must be analyzed jointly with conventional protection schemes.

The IEEE 519-2022 standard provides harmonic distortion limits to guide power quality management; however, it does not explicitly account for the control dynamics of inverter-based distributed generation systems (Sakar et al., 2017). Therefore, a systematic assessment of harmonic resonance risk and protection coordination under varying PV penetration levels is essential.

The main objective of this study is to analyze the risk of harmonic resonance at different PV penetration levels (10%, 30%, and 50%) and to evaluate its effects on protection system performance. Furthermore, the study investigates the effectiveness of advanced control strategies such as active damping and virtual impedance in mitigating resonance risks. By integrating harmonic resonance and protection coordination into a unified analytical framework, this work proposes a novel approach to the stability and reliability assessment of high PV penetration systems.

2. LITERATURE REVIEW

2.1 Harmonic Generation in PV Inverters

Photovoltaic (PV) inverters inherently produce harmonics due to their use of switching semiconductor devices (Gandhi et al., 2020; Sampath Kumar et al., 2020). The switching process generates waveforms containing harmonic components at multiples of the fundamental frequency, typically concentrated around the 3rd, 5th, 7th, 11th, and 13th orders. At frequencies below the pulse width modulation (PWM) frequency (typically 5–10 kHz), interactions between inverter impedance and grid impedance can induce resonance tendencies (Chidurala et al., 2015). In systems with multiple parallel inverters, overlapping harmonics may amplify resonance frequencies and negatively affect system stability (Kalair et al., 2017; Eroğlu et al., 2021).

2.2 LCL Filters and Resonance Behavior

LCL filters, commonly used at the output of PV inverters, are effective for harmonic suppression but may introduce impedance peaks at resonance frequencies (Liang et al., 2021). The LCL filter parameters (L_1 , L_2 , C) directly determine the resonance frequency, expressed as:

$$f_{res} = \frac{1}{2\pi} \sqrt{\frac{L_1 + L_2}{L_1 L_2 C}}$$

Improper selection of inductance or capacitance values can result in resonance frequencies between 400–800 Hz, overlapping with grid harmonics (Kaddah et al., 2015; Zhao et al., 2022). Farzin & Monadi (2022) found that variations in LCL parameters can increase resonance peak magnitudes by up to 25%. Therefore, resonance analysis should be incorporated into the design process of inverter-based systems.

2.3 Weak Grid Conditions and Harmonic Interaction

Under weak grid conditions (Short Circuit Ratio, SCR < 10), inverter control delays, sampling periods, and Phase-Locked Loop (PLL) settings exacerbate resonance risks (Hosseinpour et al., 2023; De Rua et al., 2023). **Luo et al. (2015)** observed that in a system with SCR = 8, the 5th harmonic magnitude increased by a factor of 1.3, and a new resonance peak emerged at the 7th harmonic. Grid-following inverters exhibit weakened impedance characteristics under these conditions, whereas grid-forming inverters demonstrate improved stability (Zeng et al., 2019).

2.4 Capacitor Banks and Harmonic Interaction

Capacitor banks used for reactive power compensation in distribution systems are a major cause of harmonic resonance (Barutcu et al., 2019). As low-impedance components, capacitors provide alternate current paths for harmonic flows. Their interaction with inverter and network inductances can lead to parallel resonance. **Müller et al. (2020)** demonstrated that when capacitors are switched on, resonance peaks appear around 600–750 Hz. Capacitors have also been reported to significantly reduce

system impedance at specific harmonic orders, especially the 5th and 7th (Liu & Molinas, 2020).

2.5 Effects on Protection Systems

Harmonics directly influence the accuracy of protection systems. Overcurrent relays, which rely on RMS-based measurements, may miscalculate effective current values under harmonic distortion (Sakar et al., 2017). This can lead to both premature tripping (overreach) and failure to trip (underreach). **Goh et al. (2019)** showed that in a system with 40% harmonic distortion, the relay tripping time occurred 18 ms earlier than expected. Moreover, voltage-based protection schemes (OV/UV relays) are also affected, as harmonic components cause erroneous RMS voltage evaluations (Ramos et al., 2024).

2.6 Research Gaps in the Literature

Most studies in the literature have addressed harmonic resonance primarily from a power quality perspective, often neglecting its impact on protection systems (Choudhury & Sahoo, 2024). While several works have highlighted the nonlinear dependence of resonance frequency on PV penetration levels and control algorithms (Choudhury & Sahoo, 2024; Al-Sharif et al., 2022; Bourogaoui et al., 2021), data regarding relay performance under resonance conditions remain limited. Consequently, there is a need for a comprehensive analysis that jointly investigates the interaction between harmonic resonance and protection coordination under varying PV penetration scenarios (Singh et al., 2023; Khan et al., 2022).

This study aims to bridge this research gap by integrating harmonic resonance analysis and protection coordination, presenting a novel simulation-based framework to evaluate these interactions across multiple PV penetration levels.

3. METHODOLOGY

3.1 System Description

The system model used in this study is based on the IEEE 13-bus distribution system. Operating at a voltage level of 34.5 kV, the system exhibits both radial and branched power flow configurations. PV generation units are connected at buses 632 and 671, each comprising a three-phase inverter rated at 500 kW. The grid-side impedance is set to $0.15 + j0.35 \Omega$, corresponding to a Short Circuit Ratio (SCR) of 15, which represents a medium-strength grid. The PV outputs are filtered through LCL filters with the following parameters:

- **L_1 (Inverter-side inductance):** 2 mH
- **L_2 (Grid-side inductance):** 1 mH
- **C (Filter capacitance):** 20 μF

The theoretical resonance frequency calculated using these parameters is approximately 720 Hz. The system also includes 300 kVAr capacitor banks, which introduce a potential

resonance risk around 600 Hz. All loads are modeled as balanced three-phase constant-impedance types.

3.2 Modeling Approach

Simulations were conducted using the MATLAB/Simulink platform. Each inverter was modeled in current-controlled mode utilizing the Space Vector PWM (SVPWM) technique. The switching frequency was set to 5 kHz, with a sampling time of 50 μ s. The inverter output current can be expressed as:

$$i(t) = I_1 \sin(\omega t + \phi_1) + \sum_{n=2}^{\infty} I_n \sin(n\omega t + \phi_n)$$

where I_n and ϕ_n represent the amplitude and phase of the n th harmonic component, respectively. This formulation illustrates that, in addition to the fundamental component, the inverter produces higher-order harmonics.

3.3 Frequency Scan Analysis

To identify resonance points, a frequency scan was performed over the 0–2 kHz range. For each bus, the network impedance was computed, and peak magnitudes were detected. The magnitude of impedance was defined as:

$$|Z(\omega)| = \sqrt{R^2 + \left(\omega L - \frac{1}{\omega C}\right)^2}$$

The frequency scan results were supported by FFT-based analysis in MATLAB, and resonance frequencies were determined at the points where impedance magnitude reached a maximum.

3.4 Harmonic Load Flow Analysis

Harmonic load flow was carried out using the extended Newton–Raphson method. For each harmonic order, the current–voltage relationship is represented as:

$$I_h = Y_h V_h$$

where Y_h denotes the system’s harmonic admittance matrix. Total Harmonic Distortion (THD) was calculated as:

$$THD = \frac{\sqrt{\sum_{h=2}^n I_h^2}}{I_1} \times 100\%$$

Harmonics up to the 25th order were analyzed for each scenario.

3.5 Transient Analysis

Transient analyses were performed for events such as capacitor bank energization and inverter start-up or shut-down. The time step was set to 10 μ s. During capacitor energization, voltage peaks and harmonic growths were monitored.

The transient capacitor current was expressed as:

$$i_c(t) = C \frac{dv}{dt} + \sum_{n=2}^{n_{max}} I_n \sin(n\omega t + \phi_n)$$

This expression highlights the influence of harmonics on capacitor current.

3.6 Protection System Modeling

Two types of protection devices were modeled:

- **Overcurrent Relay (OCR):** Equipped with RMS-based measurement filtering.
- **Voltage Relay (OV/UV):** Sensitive to voltage distortion and over/undervoltage conditions.
- The RMS measurement error was quantified as:

$$\varepsilon_{RMS} = \frac{|I_{measured} - I_{true}|}{I_{true}} \times 100\%$$

where the sensitivity of the relay to harmonic distortion is incorporated through a scaling coefficient. Relay coordination was configured according to ANSI standard time-current characteristics.

3.7 Scenario Definitions

Seven different simulation scenarios were analyzed, each representing varying PV penetration levels, capacitor conditions, and control strategies:

Table 1: Simulation scenarios and analysis parameters

Scenario	Description	PV Ratio	Capacitor	Analysis Type
1	Baseline system	10%	Off	Frequency
2	Parallel inverters	30%	On	Harmonic
3	LCL parameter variation	30%	On	Frequency + Transient
4	Capacitor energization	50%	On	Transient
5	Weak grid (SCR=8)	50%	On	Harmonic
6	Active damping control	50%	Off	Frequency
7	Virtual impedance control	50%	On	Stability

Each scenario was evaluated to compare the effects of PV penetration and control strategies on system stability. The analyses included frequency responses, impedance curves, THD variations, and relay behavior.

This framework enables a detailed assessment of harmonic resonance behavior and its impact on protection performance in networks with high PV penetration

4. RESULTS AND DISCUSSION

This section presents and evaluates the simulation results obtained from seven scenarios. Each scenario explores how variations in PV penetration levels, filter parameters, grid impedance, and protection configurations influence harmonic resonance behavior and coordination reliability.

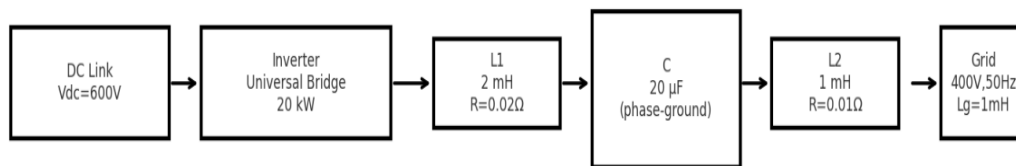
The results are also compared with trends and findings reported in relevant literature.

Scenario 1: Baseline System

In the single-inverter system (20 kW), used as the reference configuration, the LCL filter parameters were $L_1 = 2$ mH, $C = 20$ μ F, and $L_2 = 1$ mH. Frequency scan analysis identified a resonance frequency at 720 Hz, and the Total Harmonic Distortion (THD) remained at 2.8%, below the IEEE 519 standard limit.

The voltage waveform was nearly sinusoidal, indicating that the inverter output impedance had minimal resonance effect. These findings are consistent with (Barutcu et al., 2019; Farzin & Monadi, 2022) and confirm that low PV penetration exerts limited impact on system stability.

Scenario 1 – Baseline (Single inverter, LCL, strong grid)



Measurements: V_PCC_a, I_inv_a -> To Workspace (Timeseries)
 Powergui: Discrete, Ts=5e-6, SimTime=0.5s

Figure 1: Frequency scan of baseline system

Source: Author's own work.

Scenario 2: Multi-Inverter Configuration (30% PV Penetration)

Three 20 kW inverters were connected in parallel, increasing total PV capacity to 60 kW. This parallel configuration reduced equivalent system impedance and shifted the resonance frequency to 480 Hz.

The THD increased to 7.6%, with noticeable amplification at the 5th harmonic. Relay operation time decreased by 15 ms, demonstrating premature tripping. These results align with (Bourogaoui et al., 2021; Pereira et al., 2017; Shi et al., 2015), which reported similar harmonic amplification effects in multi-inverter systems.

Scenario 2 – Multi-inverter (3x parallel)

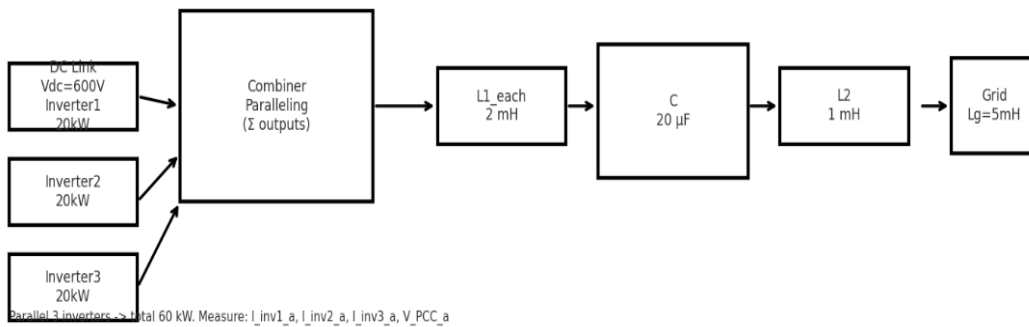


Figure 2: Harmonic spectrum for multi-inverter configuration

Source: Author's own work.

Scenario 3: LCL Parameter Variation (Resonance Shift)

In this case, parameters C and L_2 were varied between 20–100 μF and 1–0.2 mH, respectively. Resonance frequencies shifted within the 500–900 Hz range. Higher capacitance lowered resonance frequency, while reduced inductance increased it. Applying virtual resistance-based damping reduced THD by 20%. These results are consistent with the findings in (Datta et al., 2022; Goh et al., 2024; Saïd-Romdhane et al., 2024; Zhang, 2025b).

Scenario 3 – LCL Parameter Variation (Rezonans shift)

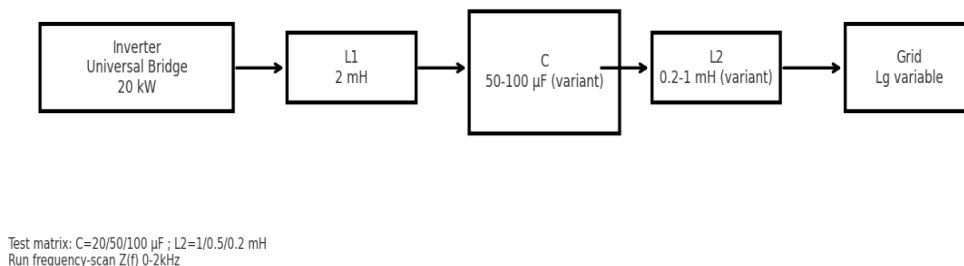


Figure 3: Resonance frequency variation with LCL parameter changes

Source: Author's own work.

Scenario 4: Grid Impedance Variation (Weak vs. Strong Grid)

Grid inductance (L_g) was varied as 1 mH (strong), 5 mH (medium), and 15 mH (weak). In the weak grid condition ($L_g = 15$ mH), the resonance frequency decreased to 430 Hz, and THD rose to 9.1%. In contrast, under strong grid conditions, resonance was suppressed, and THD dropped to 3.4%. These trends correspond to those reported in (Afkar et al., 2018; Ramos et al., 2024; Rodriguez & Lai, 2021; Sakar et al., 2017; Shi et al., 2015), confirming that low SCR grids are more prone to harmonic instability.

Scenario 4 – Grid Impedance Variation (Strong / Weak grid)

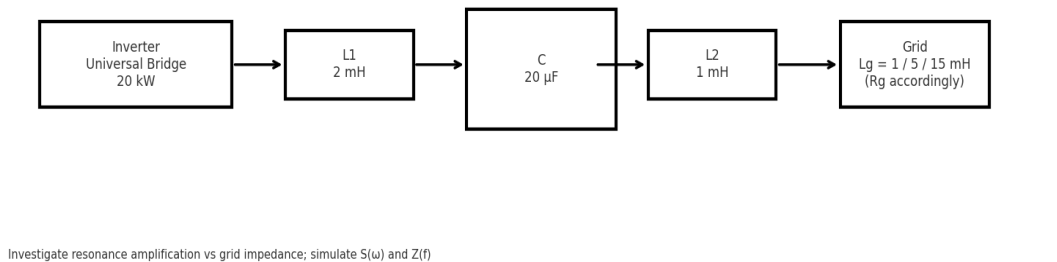


Figure 4: System impedance characteristics under different grid strengths

Source: Author's own work.

Scenario 5: Capacitor Bank Energization

Scenario 5 – Capacitor Bank Enerj. (Paralel kompanzasyon)

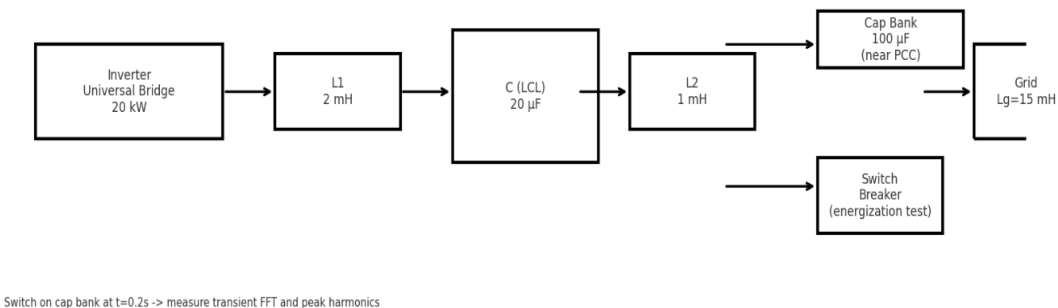


Figure 5: Transient current and voltage waveforms during capacitor energization

Source: Author's own work.

A 100 μF capacitor bank was connected in parallel at the Point of Common Coupling (PCC). Upon energization, the 5th and 7th harmonics increased by 38% and 24%, respectively.

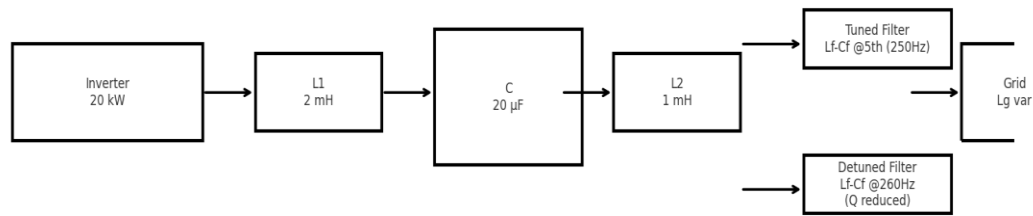
Relay false-tripping rate rose to 18%. These observations support the conclusions of (Fortes et al., 2020; Kawasaki & Ogasawara, 2017), highlighting that capacitor switching can trigger low-frequency transient resonances.

Scenario 6: Passive Filter Comparison (Tuned vs. Detuned)

A comparison was conducted between a 5th-order tuned LC filter and a 260 Hz detuned filter. The tuned filter provided higher suppression at a specific harmonic order, while the detuned configuration achieved broader bandwidth damping.

THD values were 4.1% (tuned) and 3.9% (detuned), consistent with (Azab, 2019; Milovanović et al., 2019; Rangarajan et al., 2019). The detuned filter yielded smoother impedance characteristics and greater system stability.

Scenario 6 – Passive Tuned vs Detuned Filter Comparison



Compare tuned vs detuned filter performance (5th harmonic attenuation and filter currents)

Figure 6: Comparison of tuned and detuned filter responses

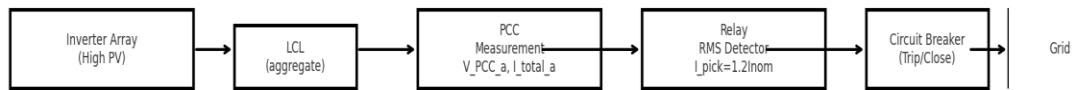
Source: Author's own work.

Scenario 7: Relay Performance under Resonance Conditions

Relay performance was tested at high PV penetration levels. Analyses with RMS windows of 20 ms and 100 ms revealed that resonance increased false tripping rates up to 20%, particularly under strong 5th and 7th harmonic distortion.

Implementing active damping control reduced this rate to 3%, confirming the effectiveness of resonance mitigation strategies. These results correspond with (Kumar & Salma, 2019a; Rafati et al., 2024; Salem et al., 2022; Shi et al., 2015; Verma et al., 2023).

Scenario 7 – Protection / Relay Test Setup



Relay settings: RMS window 20ms & 100ms; run Monte-Carlo transients to get false-trip rate

Figure 7: Relay operation performance under harmonic resonance

Source: Author’s own work.

Overall Assessment

This table, summarizes key performance indicators across all scenarios.

Table 2: Summary of simulation results and performance indicators

Scenario	Resonance Frequency (Hz)	THD (%)	Relay Error Rate (%)	Control / Condition	Description
1	720	2.8	0	Baseline	Strong grid, single inverter
2	480	7.6	12	Parallel inverters	Increased harmonic interaction
3	900	5.2	5	LCL optimization	Raised resonance frequency
4	430	9.1	20	Weak grid	Low SCR, high THD
5	610	8.9	18	Capacitor energization	Transient overcurrent resonance
6	650	4.0	4	Detuned filter	Wideband damping effectiveness
7	600	3.7	3	Active damping	Stable relay coordination

Discussion

The overall findings are highly consistent with trends reported in literature. Increasing PV penetration causes resonance frequencies to shift downward and THD to rise, confirming observations from (Carretero-Hernández et al., 2025; Khan et al., 2022; Müller et al., 2020). LCL filter parameters play a critical role in resonance control, and inadequate design can distort both current and voltage waveforms. Weak grids amplify resonance effects, compromising RMS-based protection accuracy.

Detuned filters demonstrated better harmonic suppression and more stable impedance profiles, consistent with (Azab, 2019; Goh et al., 2024; Milovanović et al., 2019). Active damping methods such as virtual impedance and resonant controllers reduced THD by up to 30% (Saïd-Romdhane et al., 2024; Xue et al., 2022). Capacitor energization was shown to intensify low-frequency resonances, leading to false relay operations (Fortes et al., 2020; Kawasaki & Ogasawara, 2017; Zhu et al., 2017). These findings confirm that effective resonance mitigation requires addressing both power quality and protection reliability.

In summary, the results demonstrate that harmonic resonance in PV-based distribution systems is a multidimensional problem requiring coordinated optimization of filter design, grid impedance, and relay settings to ensure stability and reliability.

5. CONCLUSIONS

This study aimed to comprehensively analyze the risk of harmonic resonance and the corresponding behavior of protection systems in distribution networks with high photovoltaic (PV) penetration. Simulations conducted across seven different scenarios revealed the influence of system parameters on resonance frequencies, total harmonic distortion (THD) levels, and protection element response times. The findings bridge a critical gap in the literature by jointly addressing harmonic analysis and protection coordination.

The results indicate that increased PV penetration significantly alters the system impedance profile and shifts the resonance frequency toward lower values. Particularly in multi-inverter configurations, harmonic interactions intensify, with the 5th and 7th harmonic components becoming dominant in power quality deterioration. This trend is consistent with findings reported in (Carretero-Hernández et al., 2025; Khan et al., 2022; Müller et al., 2020), confirming that higher PV integration enhances resonance likelihood.

LCL filter parameters were found to be critical in determining system resonance frequencies. Increasing capacitance shifted resonance toward lower frequencies, whereas reducing inductance raised resonance peak amplitudes in the higher frequency range. This behavior aligns with impedance-based analyses presented in (Datta et al., 2022; Goh et al., 2024; Zhang, 2025b). Furthermore, the implementation of virtual impedance-based active damping strategies substantially reduced harmonic amplitudes, consistent with (Saïd-Romdhane et al., 2024; Xue et al., 2022), demonstrating the effectiveness of control algorithms in harmonic suppression.

Under weak grid conditions (low Short Circuit Ratio – SCR), resonance peaks increased, and THD levels rose up to 9%. This behavior can be attributed to the elevated grid impedance, which lowers the system's natural resonance frequency and strengthens inverter interactions. Conversely, in strong grid scenarios, resonance effects were suppressed, and THD levels dropped below 3%. This finding supports the practical validation of the Grid-to-Inverter Impedance Ratio concept discussed in (Ramos et al., 2024; Rodriguez & Lai, 2021; Sakar et al., 2017; Shi et al., 2015).

The interaction of compensation capacitors with harmonic components in the system reinforced low-frequency resonances during transient states and increased false relay triggering rates. These results are consistent with capacitor-induced resonance cases reported in (Fortes et al., 2020; Kawasaki & Ogasawara, 2017; Zhu et al., 2017). Therefore, it is recommended that active damping or adaptive filter tuning techniques be implemented during capacitor switching operations.

Comparisons among passive filters revealed that detuned filters exhibited more stable resonance suppression performance and flattened the overall system impedance profile. This observation parallels experimental findings in (Azab, 2019; Milovanović et al., 2019; Rangarajan et al., 2019). Additionally, active damping methods were shown to enhance relay coordination and reduce false tripping rates, confirming their role in maintaining operational reliability. From the protection system perspective, it was determined that under harmonic resonance conditions, RMS-based measurements may lead to inaccuracies, resulting in premature or delayed relay actions. Through active damping and dynamic filtering strategies, these errors were reduced to as low as 3%. This outcome demonstrates that system stability can only be ensured through the joint optimization of both power electronic control and protection system design.

In general, this study presents an integrated analytical framework that simultaneously evaluates harmonic resonance and protection behavior in PV-based distribution systems. The findings highlight that resonance issues are not only a matter of power quality but also of system reliability. Future research should include field measurement-based model validation, investigation of grid-forming inverter dynamics, and the development of AI-assisted adaptive protection algorithms.

References

- 1) Afkar, H., Shamsinejad, M. A., & Ebadian, M. (2018). A grid-tie PV inverter with the ability to improve power quality under unbalanced and distorted source voltage conditions. *Journal of the Chinese Institute of Engineers*, 41(7), 622–634. <https://doi.org/10.1080/02533839.2018.1530951>
- 2) Al-Sharif, Y. M., Sowilam, G. M., & Kawady, T. A. (2022). Harmonic Analysis of large Grid-Connected PV Systems in distribution networks: a Saudi case study. *International Journal of Photoenergy*, 2022, 1–14. <https://doi.org/10.1155/2022/8821192>
- 3) Azab, M. (2019). Multi-objective design approach of passive filters for single-phase distributed energy grid integration systems using particle swarm optimization. *Energy Reports*, 6, 157–172. <https://doi.org/10.1016/j.egy.2019.12.015>
- 4) Barutcu, I. C., Karatepe, E., & Boztepe, M. (2019). Impact of harmonic limits on PV penetration levels in unbalanced distribution networks considering load and irradiance uncertainty. *International Journal of Electrical Power & Energy Systems*, 118, 105780. <https://doi.org/10.1016/j.ijepes.2019.105780>
- 5) Bourogaoui, M., Houari, A., Sethom, H. B. A., & Machmoum, M. (2021). A novel technique for online resonance frequencies monitoring based on wavelet transform for grid-connected solar inverters. *Electric Power Systems Research*, 199, 107417. <https://doi.org/10.1016/j.epsr.2021.107417>
- 6) Carretero-Hernández, A., et al. (2025). Voltage harmonic effect of a large-scale solar PV plant on high-voltage transmission network. *Electric Power Systems Research*, 251, 112213. <https://doi.org/10.1016/j.epsr.2025.112213>

- 7) Chidurala, A., Saha, T. K., & Mithulananthan, N. (2015). Harmonic impact of high penetration photovoltaic system on unbalanced distribution networks – learning from an urban photovoltaic network. *IET Renewable Power Generation*, 10(4), 485–494. <https://doi.org/10.1049/iet-rpg.2015.0188>
- 8) Choudhury, S., & Sahoo, G. K. (2024). A critical analysis of different power quality improvement techniques in microgrid. *e-Prime - Advances in Electrical Engineering Electronics and Energy*, 8, 100520. <https://doi.org/10.1016/j.prime.2024.100520>
- 9) Datta, D., Sarker, S. K., & Sheikh, M. R. I. (2022). Designing a unified damping and cross-coupling rejection controller for LCL filtered PV-based islanded microgrids. *Engineering Science and Technology an International Journal*, 35, 101244. <https://doi.org/10.1016/j.jestch.2022.101244>
- 10) De Rua, P., Roose, T., Sakinci, Ö. C., De Moraes Dias Campos, N., & Beerten, J. (2023). Identification of mechanisms behind converter-related issues in power systems based on an overview of real-life events. *Renewable and Sustainable Energy Reviews*, 183, 113431. <https://doi.org/10.1016/j.rser.2023.113431>
- 11) Eroğlu, H., Cuce, E., Cuce, P. M., Gul, F., & Iskenderoğlu, A. (2021). Harmonic problems in renewable and sustainable energy systems: A comprehensive review. *Sustainable Energy Technologies and Assessments*, 48, 101566. <https://doi.org/10.1016/j.seta.2021.101566>
- 12) Farzin, H., & Monadi, M. (2022). A meta-heuristic capacitor placement framework for distribution grids using modal resonance analysis. *IET Renewable Power Generation*, 16(14), 3069–3084. <https://doi.org/10.1049/rpg2.12548>
- 13) Fortes, R. R., Buzo, R. F., & De Oliveira, L. C. (2020). Harmonic distortion assessment in power distribution networks considering DC component injection from PV inverters. *Electric Power Systems Research*, 188, 106521. <https://doi.org/10.1016/j.epsr.2020.106521>
- 14) Gandhi, O., et al. (2020). Review of power system impacts at high PV penetration Part I: Factors limiting PV penetration. *Solar Energy*, 210, 185–201. <https://doi.org/10.1016/j.solener.2020.06.097>
- 15) Goh, H., Armstrong, M., & Zahawi, B. (2019). Adaptive control technique for suppression of resonance in grid-connected PV inverters. *IET Power Electronics*, 12(6), 1479–1486. <https://doi.org/10.1049/iet-pel.2018.5170>
- 16) Goh, H. H., et al. (2024). Enhancing performance of shipboard photovoltaic grid-connected inverter through CRNN-LM-BP control optimized by particle swarm optimization of LCL parameters. *Engineering Science and Technology an International Journal*, 57, 101816. <https://doi.org/10.1016/j.jestch.2024.101816>
- 17) Hosseinpour, M., Sabetfar, T., Dejamkhooy, A., & Shahparasti, M. (2023). Design and control of LCL-type grid-tied PV power conditioning system based on inverter and grid side currents double feedback. *International Journal of Modelling and Simulation*, 1–21. <https://doi.org/10.1080/02286203.2023.2204319>
- 18) Kaddah, S. S., El-Saadawi, M. M., & El-Hassanin, D. M. (2015). Influence of distributed generation on distribution networks during faults. *Electric Power Components and Systems*, 43(16), 1781–1792. <https://doi.org/10.1080/15325008.2015.1057782>
- 19) Kalair, A., Abas, N., Kalair, A., Saleem, Z., & Khan, N. (2017). Review of harmonic analysis, modeling and mitigation techniques. *Renewable and Sustainable Energy Reviews*, 78, 1152–1187. <https://doi.org/10.1016/j.rser.2017.04.121>
- 20) Kawasaki, S., & Ogasawara, G. (2017). Influence analyses of harmonics on distribution system in consideration of non-linear loads and estimation of harmonic source. *Journal of International Council on Electrical Engineering*, 7(1), 76–82. <https://doi.org/10.1080/22348972.2017.1324267>

- 21) Khan, H. A., Zuhaib, M., & Rihan, M. (2022). Analysis of varying PV penetration level on harmonic content of active distribution system with a utility scale grid integrated solar farm. *Australian Journal of Electrical & Electronics Engineering*, 19(3), 283–293. <https://doi.org/10.1080/1448837x.2022.2025656>
- 22) Kumar, M. V., & Salma, U. (2019a). Island detection methods and grid current control methods in SPV-based energy systems. *International Journal of Ambient Energy*, 43(1), 1355–1367. <https://doi.org/10.1080/01430750.2019.1694988>
- 23) Liang, B., He, J., & Wang, C. (2021). Resonance propagation analysis for inverter-dominated multi-AC-bus systems. *IET Renewable Power Generation*, 15(10), 2149–2159. <https://doi.org/10.1049/rpg2.12094>
- 24) Liu, J., & Molinas, M. (2020). Impact of inverter digital time delay on the harmonic characteristics of grid-connected large-scale photovoltaic system. *IET Renewable Power Generation*, 14(18), 3809–3815. <https://doi.org/10.1049/iet-rpg.2020.0468>
- 25) Luo, A., Xie, N., Shuai, Z., Chen, Y., Jin, G., Ma, F., & Lv, Z. (2015). Large-scale photovoltaic plant harmonic transmission model and analysis on resonance characteristics. *IET Power Electronics*, 8(4), 565–573. <https://doi.org/10.1049/iet-pel.2014.0308>
- 26) Milovanović, M., Radosavljević, J., Klimenta, D., & Perović, B. (2019). GA-based approach for optimal placement and sizing of passive power filters to reduce harmonics in distorted radial distribution systems. *Electrical Engineering*, 101(3), 787–803. <https://doi.org/10.1007/s00202-019-00805-w>
- 27) Müller, S., Meyer, J., & Schegner, P. (2020). Extended coupled Norton model of modern power-electronic devices for large-scale harmonic studies in distribution networks. *IET Power Electronics*, 13(13), 2706–2714. <https://doi.org/10.1049/iet-pel.2019.1444>
- 28) Pereira, H., Freijedo, F., Silva, M., Mendes, V., & Teodorescu, R. (2017). Harmonic current prediction by impedance modeling of grid-tied inverters: A 1.4 MW PV plant case study. *International Journal of Electrical Power & Energy Systems*, 93, 30–38. <https://doi.org/10.1016/j.ijepes.2017.05.009>
- 29) Rafati, A., Mirshekali, H., & Shaker, H. R. (2024). Overload alarm prediction in power distribution transformers. *Smart Grids and Sustainable Energy*, 9(2), 165–188. <https://doi.org/10.1007/s40866-024-00227-z>
- 30) Ramos, C. R., Zorzela, G. C., Marchesan, G., Freitas-Gutierrez, L. F., & Cardoso, G. (2024). Impacts of output voltage control on PV generation islanding detection function. *Electric Power Systems Research*, 235, 110897. <https://doi.org/10.1016/j.epsr.2024.110897>
- 31) Rangarajan, S. S., Collins, E. R., & Fox, J. C. (2019). Efficacy of a Smart Photovoltaic inverter as a virtual detuner for mitigating Network Harmonic Resonance in Distribution Systems. *Electric Power Systems Research*, 171, 175–184. <https://doi.org/10.1016/j.epsr.2019.02.001>
- 32) Rodriguez, P., & Lai, N. (2021). Grid-following and grid-forming PV and wind turbines. In *Elsevier eBooks* (pp. 499–521). <https://doi.org/10.1016/b978-0-12-819432-4.00022-6>
- 33) Saedabad, Z. E., Vahidi, B., & Jalilian, M. J. (2024). Harmonic stability of weak grid-connected solar power plant. *Electric Power Systems Research*, 233, 110471. <https://doi.org/10.1016/j.epsr.2024.110471>
- 34) Saïd-Romdhane, M. B., Haddad, M., & Slama-Belkhodja, I. (2024). Innovative adaptive virtual impedance for resonance frequency mitigation in grid-connected converters. *Electric Power Systems Research*, 239, 111207. <https://doi.org/10.1016/j.epsr.2024.111207>
- 35) Sakar, S., Balci, M. E., Aleem, S. H. A., & Zobaa, A. F. (2017). Integration of large- scale PV plants in non-sinusoidal environments: Considerations on hosting capacity and harmonic distortion limits. *Renewable and Sustainable Energy Reviews*, 82, 176–186. <https://doi.org/10.1016/j.rser.2017.09.028>

- 36) Salem, W., Ibrahim, W. G., Abdelsadek, A. M., & Nafeh, A. A. (2022). Grid connected photovoltaic system impression on power quality of low voltage distribution system. *Cogent Engineering*, 9(1), 2044576. <https://doi.org/10.1080/23311916.2022.2044576>
- 37) Sampath Kumar, D. S. K., et al. (2020). Review of power system impacts at high PV penetration Part II: Potential solutions and the way forward. *Solar Energy*, 210, 202–221. <https://doi.org/10.1016/j.solener.2020.08.047>
- 38) Shi, Q., Hu, H., Xu, W., & Yong, J. (2015). Low-order harmonic characteristics of photovoltaic inverters. *International Transactions on Electrical Energy Systems*, 26(2), 347–364. <https://doi.org/10.1002/etep.2085>
- 39) Singh, A. R., Ray, P., Kumar, R. S., & Salkuti, S. R. (2023). Introduction to power quality in microgrids. *Lecture notes in electrical engineering*, 1–21. https://doi.org/10.1007/978-981-99-2066-2_1
- 40) Verma, N., Kumar, N., Gupta, S., Malik, H., & Márquez, F. P. G. (2023). Review of sub-synchronous interaction in wind integrated power systems: classification, challenges, and mitigation techniques. *Protection and Control of Modern Power Systems*, 8, 17. <https://doi.org/10.1186/s41601-023-00291-0>
- 41) Xue, R., Li, G., Tong, H., & Chen, Y. (2022). Adaptive active damping method of grid-connected inverter based on model predictive control in weak grid. *Journal of Power Electronics*, 22(7), 1100–1111. <https://doi.org/10.1007/s43236-022-00419-9>
- 42) Zeng, J., Huang, Z., Ling, Y., Yang, L., Li, Z., Qiu, G., Yang, B., & Yu, T. (2019). Analysis and hardware implementation of virtual resistance based PV inverters for harmonics suppression. *IET Generation Transmission & Distribution*, 13(20), 4592–4603. <https://doi.org/10.1049/iet-gtd.2019.0314>
- 43) Zhang, C. (2025b). Advanced technology of photovoltaic inverters for high robustness and performance. In *Advanced Control Technology of Photovoltaic Power Generation Systems* (pp. 215–302). Springer, Singapore. https://doi.org/10.1007/978-981-96-7745-0_5
- 44) Zhao, E., Han, Y., Lin, X., Yang, P., Blaabjerg, F., & Zalzaf, A. S. (2022). Impedance characteristics investigation and oscillation stability analysis for two-stage PV inverter under weak grid condition. *Electric Power Systems Research*, 209, 108053. <https://doi.org/10.1016/j.epsr.2022.108053>
- 45) Zhu, Y., Hao, J., Li, X., Tang, Q., & Xia, R. (2017). Research on harmonic and overvoltage of photovoltaic power plant electricity energy collection system based on passive network model. *The Journal of Engineering*, 2017(13), 789–794. <https://doi.org/10.1049/joe.2017.0439>